Article

Reversible Surface Oxidation and Efficient Luminescence Quenching in Semiconductor Single-Wall Carbon Nanotubes

Gordana Dukovic, Brian E. White, Zhiyong Zhou, Feng Wang, Steffen Jockusch, Michael L. Steigerwald, Tony F. Heinz, Richard A. Friesner, Nicholas J. Turro, and Louis E. Brus

J. Am. Chem. Soc., **2004**, 126 (46), 15269-15276• DOI: 10.1021/ja046526r • Publication Date (Web): 30 October 2004

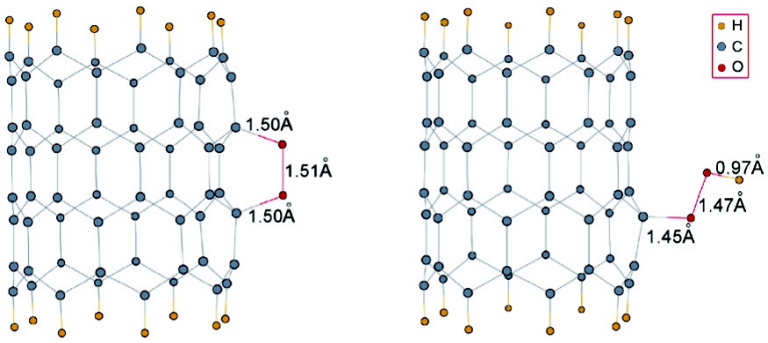

More About This Article

Additional resources and features associated with this article are available within the HTML version:

- Supporting Information
- Links to the 33 articles that cite this article, as of the time of this article download
- Access to high resolution figures
- Links to articles and content related to this article
- Copyright permission to reproduce figures and/or text from this article

View the Full Text HTML

J|A|C|S
ARTICLES
Published on Web 10/30/2004

Reversible Surface Oxidation and Efficient Luminescence Quenching in Semiconductor Single-Wall Carbon Nanotubes

Gordana Dukovic,[†] Brian E. White,[†] Zhiyong Zhou,[†] Feng Wang,[‡] Steffen Jockusch,[†] Michael L. Steigerwald,[†] Tony F. Heinz,[‡] Richard A. Friesner,[†] Nicholas J. Turro,[†] and Louis E. Brus*[,†]

Contribution from the Department of Chemistry, Columbia University, 3000 Broadway, New York, New York 10027, and Department of Physics, Columbia University, 538 West 120th Street, New York, New York 10027

Received June 11, 2004; E-mail: brus@chem.columbia.edu

Abstract: We have investigated reversible single-wall carbon nanotube (SWNT) oxidation by quantitative analysis of the oxide-induced absorption bleaching and luminescence quenching at low pH. These data, in combination with DFT structure calculations, suggest that the nanotube oxide is a 1,4-endoperoxide. At low pH, the endoperoxide protonates to create a hydroperoxide carbocation, introducing a hole in the SWNT valence band. Nanotube luminescence is extremely sensitive to quenching by hole-doping, while the absorption is relatively robust.

Introduction

One-dimensional, aromatic single-wall carbon nanotubes (SWNTs) have unique electronic and physical properties that have attracted widespread attention.[1] More than 100 crystalline structural types differing in diameter and chiral angle are possible; one-third of these are metallic and two-thirds are low-band-gap semiconductors.[1] In electrical measurements, SWNTs show very high electron mobility, and in the absence of defects, electrons can propagate without scattering or heat production over lengths of micrometers.[2] The current is carried by π electrons whose structure is essentially predicted by simple $\pi-\pi^*$ Hückel theory.[3]

The one-dimensional density of electronic states (DOS) of SWNTs is characterized by sharp van Hove singularities. The resulting $\pi-\pi^*$ optical transitions between filled and empty singularities are strongly allowed. Upon photoexcitation, semiconducting nanotubes exhibit band-gap photoluminescence in the near-IR;[4−8] the corresponding excitation spectra have been used to correlate optical transition energies with nanotube structures.[4] The high electrical conductivity and photoconductivity of SWNTs suggests that the optically excited electronic states are highly mobile and likely to be sensitive to quenching. Indeed, recent studies report that a small number of extra holes or electrons in a 400-nm-long tube can quench excited states through a nonradiative Auger recombination mechanism.[9] This process is sufficiently fast to compete with the very rapid trapping processes that limit the lifetime of an excited electron−hole pair in the radiative state to ∼10 ps.[10]

While it is well known that polycondensed molecules with large π-electron systems are sensitive to oxygen, especially in its excited $^1\Delta$ state, which lies 1.07 eV above the ground $^3\Sigma$ state,[11] little is known about the corresponding oxidation of SWNT sidewalls. The experimentally measured binding energy of $^3\Sigma$ O_2 to nanotube bundles (0.19 eV) is 55% higher than that of graphite, but still in the range of physisorption.[12,13] Exposure of nanotubes to UV light in the presence of oxygen has been shown to significantly accelerate nanotube oxidation, suggesting the involvement of $^1\Delta$.[14] Several theoretical papers predict that the ground-state $^3\Sigma$ oxygen indeed interacts weakly with nanotube sidewalls, while the $^1\Delta$ state is expected to bind to them.[14−20] Nanotube samples are expected to contain fullerenes,[19] which are known singlet-oxygen sensitizers,[21] making $^1\Delta$ a

[†] Department of Chemistry, Columbia University.
[‡] Department of Physics, Columbia University.

(1) Odom, T. W.; Huang, J. L.; Kim, P.; Lieber, C. M. *J. Phys. Chem. B* **2000**, *104*, 2794−2809.
(2) Javey, A.; Guo, J.; Wang, Q.; Lundstrom, M.; Dai, H. J. *Nature* **2003**, *424*, 654−657.
(3) Saito, R.; Dresselhaus, G.; Dresselhaus, M. S. *Physical properties of carbon nanotubes*; Imperial College Press: London, 1998.
(4) Bachilo, S. M.; Strano, M. S.; Kittrell, C.; Hauge, R. H.; Smalley, R. E.; Weisman, R. B. *Science* **2002**, *298*, 2361−2366.
(5) Lefebvre, J.; Frasier, J. M.; Finnie, P.; Homma, Y. *Phys. Rev. B* **2004**, *69*, 075403.
(6) Lefebvre, J.; Homma, Y.; Finnie, P. *Phys. Rev. Lett.* **2003**, *90*, 217401.
(7) Hartschuh, A.; Pedrosa, H. N.; Novotny, L.; Krauss, T. D. *Science* **2003**, *301*, 1354−1356.
(8) O'Connell, M. J.; Bachilo, S. M.; Huffman, C. B.; Moore, V. C.; Strano, M. S.; Haroz, E. H.; Rialon, K. L.; Boul, P. J.; Noon, W. H.; Kittrell, C.; Ma, J. P.; Hauge, R. H.; Weisman, R. B.; Smalley, R. E. *Science* **2002**, *297*, 593−596.
(9) Wang, F.; Dukovic, G.; Knoesel, E.; Brus, L.; Heinz, T. *Phys. Rev. B*, accepted.
(10) Wang, F.; Dukovic, G.; Brus, L. E.; Heinz, T. F. *Phys. Rev. Lett.* **2004**, *92*, 177401.
(11) Aubry, J. M.; Pierlot, C.; Rigaudy, J.; Schmidt, R. *Acc. Chem. Res.* **2003**, *36*, 668−675.
(12) Ulbricht, H.; Moos, G.; Hertel, T. *Phys. Rev. B* **2002**, *66*, 075404.
(13) Ulbricht, H.; Moos, G.; Hertel, T. *Surf. Sci.* **2003**, *532*, 852−856.
(14) Savage, T.; Bhattacharya, S.; Sadanadan, B.; Gaillard, J.; Tritt, T. M.; Sun, Y. P.; Wu, Y.; Nayak, S.; Car, R.; Marzari, N.; Ajayan, P. M.; Rao, A. M. *J. Phys.: Condens. Matter* **2003**, *15*, 5915−5921.
(15) Sorescu, D. C.; Jordan, K. D.; Avouris, P. *J. Phys. Chem. B* **2001**, *105*, 11227−11232.
(16) Froudakis, G. E.; Schnell, M.; Muhlhauser, M.; Peyerimhoff, S. D.; Andriotis, A. N.; Menon, M.; Sheetz, R. M. *Phys. Rev. B* **2003**, *68*, 115435.
(17) Giannozzi, P.; Car, R.; Scoles, G. *J. Chem. Phys.* **2003**, *118*, 1003−1006.
(18) Mann, D. J.; Hase, W. L. *Phys. Chem. Chem. Phys.* **2001**, *3*, 4376−4383.

possible oxidation agent. The existence of surface oxides was implied in early resonance Raman experiments, where heating tubes to several hundred degrees Celsius appeared to remove surface-adsorbed species and significantly improved the resonance Raman spectra.[22,23] In metallic tubes, Yu and Brus interpreted this reversible effect as a shift in the Fermi level due to holes from electronegative surface species.[22] Treatment with strong oxidizing acids is also known to partially oxidize the nanotube sidewalls[24] and bleach the band-gap optical absorption of semiconducting nanotubes.[25]

O'Connell et al. discovered a procedure for exfoliating nanotube bundles and creating micellar suspensions of submicrometer sections of isolated SWNTs.[8] They found that only isolated semiconductor tubes (not tubes in bundles) photoluminesce. Photoluminescence from individual SWNTs grown directly on substrates by chemical vapor deposition has also been reported.[5,6] Strano et al. observed that the SWNT band-gap optical absorption is bleached at low pH values in sodium dodecyl sulfate (SDS) micellar suspensions.[26] This is accompanied by complete loss of luminescence. If oxygen is desorbed by UV irradiation, bleaching disappears and the luminescence recovers. The authors propose that a protonated surface oxide of unknown structure localizes an SWNT electron, thus creating a hole in the valence band. A pH-dependent bleaching has also been observed in DNA-solubilized tubes.[27]

In this paper, we quantitatively study the reversible oxidation of SWNT sidewalls and the associated luminescence quenching at low pH. We monitor the thermal oxide decomposition by recording the evolution of the luminescence during heating. Controlled reoxidation using 1,4-dimethylnaphthalene-1,4-endoperoxide as a source of $^1\Delta$ oxygen shows that the presence of only a few ($\leq$10) surface oxide species per 400-nm-long carbon nanotube (ca. 20 000 aromatic rings) is sufficient to quench the luminescence. In contrast to the observed luminescence quenching, we estimate that roughly 250 holes per 400 nm tube are necessary to bleach the corresponding band-gap transition in absorption. Electronic structure calculations suggest that the surface oxide made by $^1\Delta$ attack is a 1,4-endoperoxide species oriented along the SWNT axis, which in the presence of H^+ transforms into a hydroperoxide carbocation. It is this protonated species that hole-dopes the nanotube and affects its optical properties. We conclude that the excited state produced in a SWNT by absorption of a photon is remarkably sensitive to quenching along the entire length of the nanotube.

Experimental and Computational Methods

Sample Preparation. Air-equilibrated SWNT suspensions in poly(maleic acid/octyl vinyl ether) (PMAOVE; Figure 1a) were prepared using a modification of the method first reported by O'Connell et al. for SDS.[8] Commercially available[28] SWNTs grown by the high-pressure CO (HiPCO) method[29] were mixed with a 1% w/v solution of PMAOVE in water. The mixture was subjected to vigorous sonication and centrifugation at 110000*g*. The sonication is thought to exfoliate nanotube bundles, while centrifugation removes the remaining bundles and all other impurities (such as catalytic and carbonaceous particles, and MWNTs).[8] Nanotube suspensions consisted of short isolated SWNTs, as confirmed by AFM measurements of the nanotubes on a substrate.[10] The average nanotube length was ~400 nm.[10] The natural pH of PMAOVE solutions at this concentration is ~3. To obtain the spectra shown in Figure 1, the pH was adjusted with 13 M NaOH. The initial sample preparation was carried out under the air atmosphere, and no efforts were made to exclude oxygen.

Spectroscopic Methods. Absorption spectra were recorded on a Perkin-Elmer Lambda 19 UV−vis−NIR spectrophotometer. Steady-state luminescence spectra were recorded on a Fluorolog-2 spectrometer (Jobin Yvon Inc.) in conjunction with a near-IR sensitive PMT (H9170-45; Hamamatsu). The excitation source was a diode laser (CQL784/D4; Philips; 22 mW; irradiation intensity 35 mW/cm^2) emitting at 785 nm, powered by a LD1100 constant power laser driver (Thorlabs Inc.). The emission intensity was linearly proportional to the excitation intensity.

Oxygen Desorption. Oxygen desorption experiments were carried out in a quartz cuvette equipped with a reflux condenser. Argon was introduced via stainless steel needles through rubber septa. Air-saturated SWNT suspensions in PMAOVE solution at pH 3 were heated to 97 °C under argon and were periodically briefly cooled to room temperature to record the photoluminescence spectra.

SWNT Reoxidation. SWNT samples were reoxidized at room temperature by 1,4-dimethylnaphthalene-1,4-endoperoxide (DMN-O_2). Deoxygenated SWNT micellar solution was added to an argon-purged airtight cuvette containing the endoperoxide. The endoperoxide was delivered from a dichloromethane solution, and the solvent was allowed to evaporate under Ar before the SWNT suspensions were added. All transfer of solutions was done under Ar to minimize contamination from the atmospheric oxygen. Luminescence spectra were recorded after 15 h, which corresponds to 3 half-lives of the endoperoxide. All endoperoxide concentrations were below the solubility limit of oxygen in water.

Density Functional Theory (DFT) Methods. Static B3LYP DFT calculations with an atom-centered basis and complete geometrical optimization were performed with Jaguar 5.0.[30] Application of these methods to SWNTs has been described and calibrated in an extensive study of (5,5) SWNT short sections with the ends of the nanotubes terminated by H atoms.[31]

Results

Choice of Surfactant. We found that aqueous suspensions of SWNTs using poly(maleic acid/octyl vinyl ether) (PMAOVE) as the surfactant are extremely robust under a wide range of conditions. In particular, they are stable to flocculation in the pH range 3−12, and at temperatures up to 97 °C. In comparison, SWNT suspensions in SDS as the surfactant flocculate at high pH and high temperatures. The repeat unit structure of PMAOVE is shown as an inset in Figure 1a. In water solution, octyl side chains form intramolecular hydrophobic domains, similar to the inner regions of traditional micelles, while the acid groups form an interface with water.[32] We expect that the hydrophobic side

(19) Chan, S. P.; Chen, G.; Gong, X. G.; Liu, Z. F. *Phys. Rev. Lett.* **2003**, *90*, 086403.
(20) Grujicic, M.; Cao, G.; Rao, A. M.; Tritt, T. M.; Nayak, S. *Appl. Surf. Sci.* **2003**, *214*, 289−303.
(21) Foote, C. S. *Top. Curr. Chem.* **1994**, *169*, 347−363.
(22) Yu, Z. H.; Brus, L. E. *J. Phys. Chem. A* **2000**, *104*, 10995−10999.
(23) Corio, P.; Santos, P. S.; Pimenta, M. A.; Dresselhaus, M. S. *Chem. Phys. Lett.* **2002**, *360*, 557−564.
(24) Kuznetsova, A.; Popova, I.; Yates, J. T.; Bronikowski, M. J.; Huffman, C. B.; Liu, J.; Smalley, R. E.; Hwu, H. H.; Chen, J. G. G. *J. Am. Chem. Soc.* **2001**, *123*, 10699−10704.
(25) Hennrich, F.; Wellmann, R.; Malik, S.; Lebedkin, S.; Kappes, M. M. *Phys. Chem. Chem. Phys.* **2003**, *5*, 178−183.
(26) Strano, M. S.; Huffman, C. B.; Moore, V. C.; O'Connell, M. J.; Haroz, E. H.; Hubbard, J.; Miller, M.; Rialon, K.; Kittrell, C.; Ramesh, S.; Hauge, R. H.; Smalley, R. E. *J. Phys. Chem. B* **2003**, *107*, 6979−6985.
(27) Zheng, M.; Jagota, A.; Semke, E. D.; Diner, B. A.; Mclean, R. S.; Lustig, S. R.; Richardson, R. E.; Tassi, N. G. *Nat. Mater.* **2003**, *2*, 338−342.
(28) Carbon Nanotechnologies Inc., Houston, TX.
(29) Nikolaev, P.; Bronikowski, M. J.; Bradley, R. K.; Rohmund, F.; Colbert, D. T.; Smith, K. A.; Smalley, R. E. *Chem. Phys. Lett.* **1999**, *313*, 91−97.
(30) Jaguar 5.0, Schrodinger, L.L.C., Portland, OR, 1991−2003.
(31) Zhou, Z. Y.; Steigerwald, M.; Hybertsen, M.; Brus, L.; Friesner, R. A. *J. Am. Chem. Soc.* **2004**, *126*, 3597−3607.
(32) Qiu, Q.; Lou, A.; Somasundaran, P.; Pethica, B. A. *Langmuir* **2002**, *18*, 5921−5926.

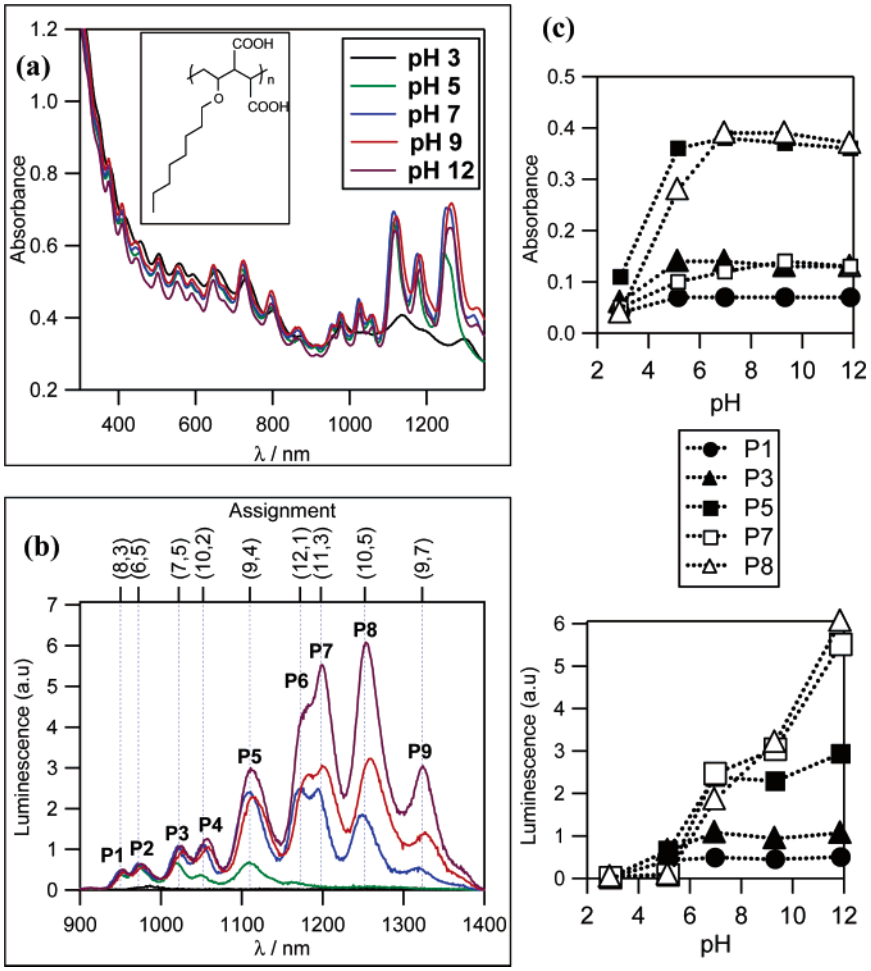

Figure 1. (a) pH dependence of SWNT absorption spectra in air-saturated solutions. Inset: Repeat unit structure of PMAOVE. (b) pH dependence of SWNT photoluminescence. The nine photoluminescence peaks are identified as P1 through P9, each corresponding to emission from a particular nanotube structure (assignments[4] on top axis). The diameter of the nanotubes increases from left to right. (c) Peak intensities as a function of pH for absorption (upper panel) and photoluminescence (lower panel).

chains associate with the SWNT and the acid group with the bulk aqueous phase, as is the case with SDS micelles.[8]

pH Dependence of Absorption and Luminescence Spectra before Removal of O_2. Figure 1a shows the absorption spectra of air-saturated SWNT suspensions at different pH values. The spectral region between 900 and 1400 nm contains the semiconductor band-gap transitions.[3] We observe a pronounced pH dependence very similar to that in SDS suspensions.[26] The pH effect is even more pronounced in the photoluminescence spectra (Figure 1b). Each luminescence peak corresponds to a different tube structure identified in Table 1; SWNT diameter increases with increasing wavelength. Absorption and luminescence intensities decrease with decreasing pH. This decrease is fastest for the largest-diameter tubes. Figure 1c illustrates that, for a given nanotube structure, the luminescence quenching happens at lower H^+ concentrations than the absorption bleaching. The absorption bleaching curves in Figure 1c resemble simple acid−base titration curves with an intensity independent of acidity above pH 7. The luminescence behavior is more complex, and for the largest-diameter tubes luminescence intensity appears to still be increasing at pH 12. It is useful to compare the pH values at which absorption and luminescence are at half of their maximum values for a given nanotube species. The difference between the two depends strongly on diameter. For peak 1 (smallest diameter), the value for absorption is pH 4.0, and pH 4.3 for luminescence; for peak 5, on the other hand, the value for absorption is pH 4.15, but pH 6.03 for luminescence. This difference between the pH effect in bleaching and luminescence has not been previously reported.

Table 1. O_2 Desorption Rate Constants Measured by Luminescence Recovery[a]

peak	peak position (nm)	assignment[b]	diameter (nm)	t_0 (min)	rate constant (h^{-1})	E_a (eV)
P1	962	(8,3)	0.78	5	3.8	1.17
P2	984	(6,5)	0.76	5	5.1	1.16
P3	1032	(7,5)	0.83	15	4.6	1.16
P4	1064	(10,2)	0.88	15	3.6	1.17
P5	1118	(9,4)	0.91	15	3.2	1.17
P6	1192	(12,1)	0.99	25	2.1	1.18
P7	1204	(11,3)	1.01	25	2.0	1.19
P8	1264	(10,5)	1.05	30	1.9	1.19
P9	1324	(9,7)	1.10	40	1.8	1.19

[a] t_0 is the induction period; other symbols have their standard meanings. [b] From ref 4.

Oxygen Desorption Kinetics. SWNT suspensions are prepared and initially characterized in air at room temperature. When we heat the essentially nonluminescent solution (pH 3) to 97 °C under Ar, both the absorption and luminescence spectra

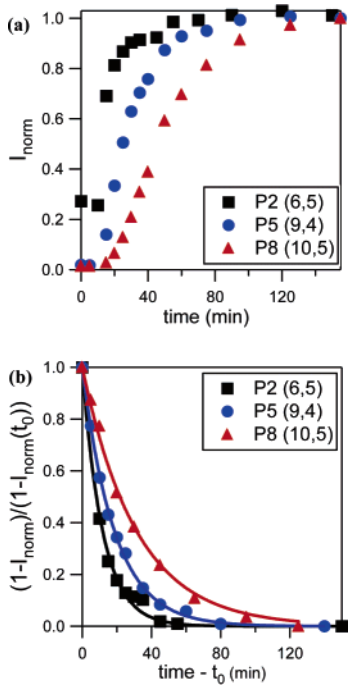

Figure 2. Oxygen desorption kinetics measured by luminescence recovery at 97 °C. (a) Normalized luminescence intensity ($I_{norm} = I/I_{max}$) for three luminescent SWNT species as a function of time under argon. After the induction period t_0, the luminescence increases over a period of 2 h. (b) Using a unimolecular decomposition model A → B, where A is completely nonluminescent and B is luminescent, the luminescence recovery data are fit to the expression $(1 - I_{norm}(t - t_0)/1 - I_{norm}(t_0)) = e^{-k(t-t_0)}$, where k is the decomposition rate constant. Solid lines are the fit curves. Values of t_0 and k are listed in Table 1.

return to those seen for air-saturated, pH 9 samples. We attribute this to removal of protonated sidewall oxide species. The thermal deoxygenation method, unlike UV photodesorption,[26] allows us to directly measure the oxygen desorption kinetics for each nanotube structure represented in the luminescence spectra. Figure 2a shows the luminescence intensity for three nanotube species as a function of heating time at 97 °C. Within 2.5 h, all of the luminescence peaks reach their maximum values. The recovered luminescence is stable for days at 25 °C under Ar. If the pH 3 solution is heated under O_2, the luminescence intensity does not increase at all. In addition, heating of high-pH SWNT suspensions under Ar does not result in significant changes in luminescence intensity. These control experiments confirm that both O_2 and H^+ are necessary for absorption bleaching and luminescence quenching and that the responsible species is likely a protonated, not neutral, oxide.

The luminescence recovery curves (Figure 2a) are complex. Phenomenologically, they consist of an induction period followed by a rise that is fit well by first-order kinetics. The fits are illustrated in Figure 2b. In Table 1, we give the best two-parameter fit (induction time, t_0, and rate constant, k) for each nanotube structure. It is apparent that the luminescence recovery is fastest and the induction period the shortest for the smallest-diameter tubes. The apparent first-order kinetics is consistent with unimolecular decomposition of a surface species after an initial induction period. We can obtain the upper limit for activation energy (E_a) within the context of unimolecular decomposition theory[33] by setting $\Delta S^{\ddagger}$ equal to zero. The values, also shown in Table 1, are around 1.2 eV. The upper limit refers to a decomposition with a concerted transition state,[34] while a more complicated mechanism should have a lower E_a.

Reoxidation of SWNT Sidewalls. SWNT oxide desorption is completely reversible by re-admission of molecular oxygen. If air is admitted to the deoxygenated pH 3 sample at 25 °C, the luminescence intensity decreases again on a time scale of days. Bubbling of oxygen through solutions of deoxygenated nanotubes eventually results in luminescence quenching, but the kinetics of the process was not reproducible, presumably due to the common sensitivity of aromatic molecule oxidation to light and heat. By contrast, reproducible results were obtained when micromolar amounts of oxygen were added using 1,4-dimethylnaphthalene-1,4-endoperoxide (DMN-O_2), which is a standard source of $^1\Delta$ O_2.[35] At 23 °C, this molecule decomposes into excited oxygen and the parent naphthalene (DMN) with a half-life of 5 h[36] and with yield of 76%.[34] We attribute the reproducible luminescence quenching at low concentration to the reaction of $^1\Delta$ oxygen with the SWNT.

Figure 3a illustrates luminescence quenching at pH 3 (15 h after addition of the endoperoxide) as a function of DMN-O_2 concentration. Luminescence from larger-diameter tubes is quenched at lower concentrations of DMN-O_2, indicating, in accordance with the findings for oxygen removal, that the larger-diameter tubes are more sensitive to oxygen. In a control experiment, a large excess of 1,4-dimethylnaphthalene (0.3 mM) itself did not quench the SWNT emission. The remarkable observation is that DMN-O_2 at a concentration of 3.3 μM quenches ~80% of the total SWNT luminescence. Importantly, at the same concentration, the endoperoxide does not bleach the absorption transitions, as shown in Figure 3b.

Estimate of SWNT Concentration. The total length of semiconducting carbon nanotubes (per milliliter of solution) is estimated from the measured optical absorption. We do this by considering integrated deoxygenated band-gap absorption using the oscillator strength calculated by Perebeinos et al.[37] and its relation to the absorptivity A (per centimeter of path length):[38]

$$\frac{1}{3}f = \frac{4m_e\epsilon_0 cn}{[C]e^2h}\int A\,dE$$

Here, n is the index of refraction of the solution, and m_e, ϵ_0, c, e, and h are the usual physical constants. [C] is the total number of carbon atoms in SWNTs per milliliter. The factor of 1/3 takes into account the orientation of absorption along the nanotube length.[39] Using $E_{exc} = 0.99$ eV (consistent with the finding of Bachilo et al. that the average diameter of semiconducting tubes in HiPCO samples is 0.93 nm,[4] corresponding to the (10,3) tube), this gives [C] = 7×10^{16} C atoms/mL, or 7×10^{14} nm of total nanotube length per milliliter. As our average nanotube length is 400 nm, the semiconducting SWNT concentration is 3 nM (60 μM of six-membered aromatic rings). The peak band-

(33) Laidler, K. J. *Chemical kinetics*, 3rd ed.; Harper & Row: New York, 1987.
(34) Turro, N. J.; Chow, M. F.; Rigaudy, J. *J. Am. Chem. Soc.* **1981**, *103*, 7218−7224.
(35) Gunther, G.; Lemp, E.; Zanocco, A. L. *J. Photochem. Photobiol. A* **2002**, *151*, 1−5.
(36) Wasserman, H. H.; Larsen, D. L. *J. Chem. Soc., Chem. Commun.* **1972**, 253−254.
(37) Perebeinos, V.; Tersoff, J.; Avouris, P. *Phys. Rev. Lett.* **2004**, *92*, 257402.
(38) p't Hooft, G. W.; Van der Poel, W. A. J. A.; Molenkamp, L. W.; Foxon, C. T. *Phys. Rev. B: Condens. Matter Mater. Phys.* **1987**, *35*, 8281−8284.
(39) Duesberg, G. S.; Loa, I.; Burghard, M.; Syassen, K.; Roth, S. *Phys. Rev. Lett.* **2000**, *85*, 5436−5439.

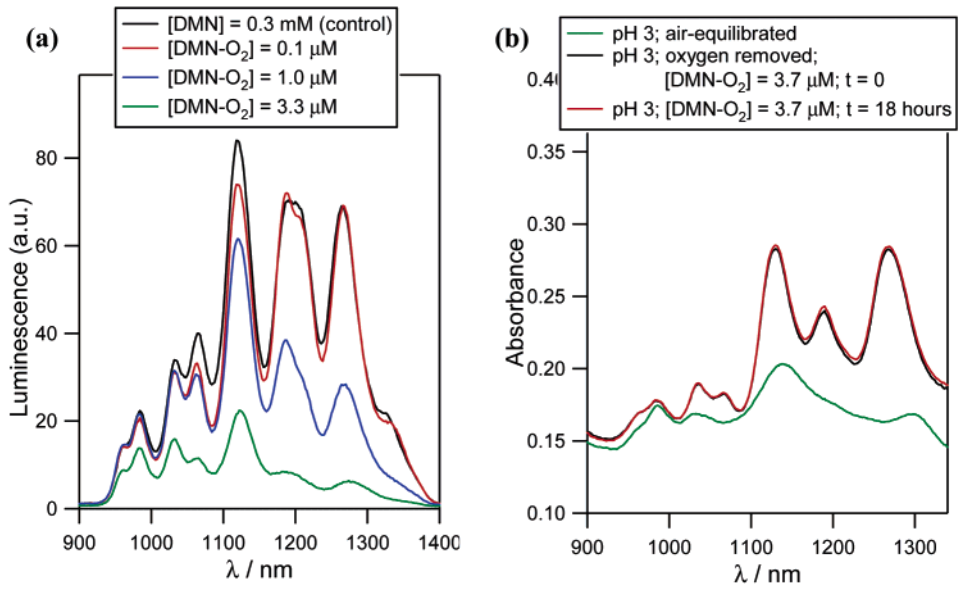

Figure 3. Reoxidation at pH 3 after removal of sidewall oxides. (a) Luminescence quenching as a function of 1,4-dimethylnaphthalene-1,4-endoperoxide (DMN-O_2) concentration. Larger-diameter tubes are more sensitive to the released $^1\Delta$ O_2. Integrated photoluminescence intensity decreases to ~20% of its maximum intensity when [DMN-O_2] = 3.3 μM. (b) Absorption intensity before, immediately after, and 18 h after addition of 3.7 μM DMN-O_2. Whereas DMN-O_2 at this concentration significantly quenches SWNT luminescence, it does not reduce the absorption intensity.

gap absorption cross section is about 4×10^{-13} cm^2/nanotube. In chemical units, the SWNT extinction coefficient $\epsilon_{max} = 2 \times 10^8$ cm^{-1} M^{-1} (11 000 cm^{-1} M^{-1} for six-membered aromatic rings). In comparison, the values of ϵ_{max} for $\pi-\pi^*$ transitions of benzene and anthracene are 200 and 10 000 cm^{-1} M^{-1}, respectively.[40]

Discussion

Quantitative Analysis of Luminescence Quenching and Absorption Bleaching. The measured luminescence quenching as a function of DMN-O_2 concentration enables us to obtain a rough estimate of the number of surface oxide species per nanotube necessary for luminescence quenching. The hydrophobic DMN-O_2 molecules should reside inside the PMAOVE micelles. These take up 1% of the total solution volume, so that the effective micellar concentration of DMN-O_2 is about 0.33 mM at the 3.3 μM overall concentration necessary for quenching. We assume that the hydrophobic DMN-O_2 molecules are randomly distributed in the micelles. In principle, the molecules might preferentially adsorb on the SWNT, but a Langmuir adsorption isotherm calculation[41] (using a binding energy of 0.22 eV predicted for naphthalene on graphite[42]) shows that DMN-O_2 surface binding is negligible at these low concentrations. A PMAOVE micelle containing a SWNT might be about 400 nm long with a 1.5 nm radius. At 0.33 mM DMN-O_2 effective micelle concentration, the average micelle occupancy is 0.6. Thus, even if the $^1\Delta$ O_2 yield from DMN-O_2 were 100%, less than one $^1\Delta$ oxygen molecule should be available for immediate reaction inside the micelle.

It is possible that $^1\Delta$ O_2 could diffuse from other nearby micelles to react with the SWNT. The $^1\Delta$ O_2 molecules liberated from 3.3 μM DMN-O_2 are separated by an average distance of 87 nm in solution (if we envision them distributed homogeneously on a cubic lattice). If $^1\Delta$ O_2 is to diffuse from one micelle to the next, it must pass through water, where its lifetime is 4.2 μs,[43] corresponding to a diffusion length of 114 nm. Taking into consideration this diffusive motion, we estimate that still only a small number ($\leq$10) of $^1\Delta$ oxygen molecules should survive long enough to reach and react with a given 400 nm long SWNT. If we assume that each surface oxide at pH 3 creates a free mobile hole in the SWNT, this result is consistent with the observation that just a few free electrons or holes per 400 nm SWNT quench the nanotube luminescence by Auger recombination.[9] This result also qualitatively explains the induction period in the kinetics of oxygen desorption (Figure 2a). During the decay period, the presence of multiple holes quenches the luminescence by Auger recombination, and only when there are a few holes present do we start to see the luminescence recover. For this explanation to be quantitative, the last oxygen species to desorb must have much longer residence times on nanotube sidewalls than the O_2 molecules that desorb first.

The bleaching of the band-gap optical absorption at pH 3 exhibits a very different sensitivity to the presence of surface oxide. We estimate that about 250 valence band holes are necessary to bleach the band-gap absorption in a 400 nm long tube (see Supporting Information). This value is more than an order of magnitude greater than the experimental number of holes necessary for luminescence quenching. The greater number of holes necessary for bleaching is supported by the experimental observation that the luminescence is quenched at a lower H^+ concentration than necessary for absorption bleaching (Figure 1c).

Surface Oxide Structure and Chemical Reaction Mechanism. The reversible interaction of $^1\Delta$ oxygen with large π electron polycondensed molecules almost universally forms a 1,4-endoperoxide, in which O_2 adds across a C_6-hexagon. More than 400 such organic endoperoxides have been described.[44] In

(40) Turro, N. J. *Modern Molecular Photochemistry*; University Science Books: Mill Valley, CA, 1991.
(41) Davis, H. T. *Statistical Mechanics of Phases, Interfaces, and Thin Films*; Wiley-VCH: New York, 1996; eq 3.6.7.
(42) O'Dea, A. R.; Smart, R. S.; Gerson, A. R. *Carbon* **1999**, *37*, 1133−1142.
(43) Schmidt, R.; Afshari, E. *Ber. Bunsen-Ges.* **1992**, *96*, 788−794.

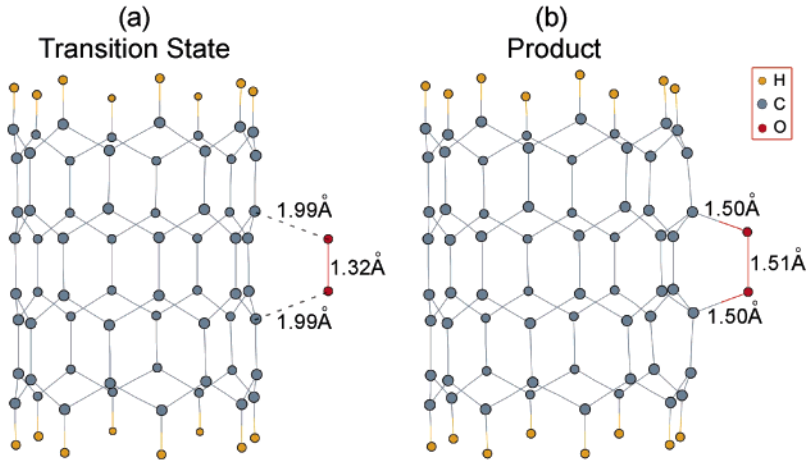

Figure 4. Calculated structures for O_2 addition to a short semiconductor SWNT section as described in the text: (a) the transition state along the path for O_2 dissociation; (b) the stable endoperoxide.

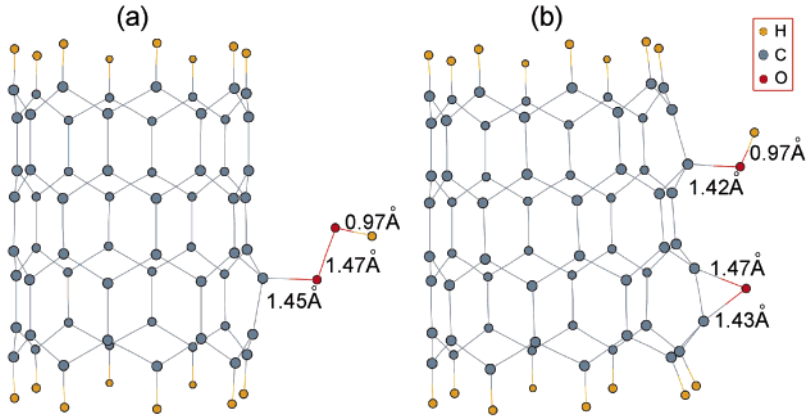

Figure 5. Calculated protonated endoperoxide structures as described in the text. The hydroperoxide in (a) is the dominant converged DFT structure; the epoxide in (b) was obtained after a few runs.

electronic structure calculations on these species, larger binding energies (up to 1 eV with respect to $^3\Sigma$ O_2) correlate with smaller initial aromatic $\pi-\pi^*$ HOMO−LUMO gaps and increased delocalization.[45] Mann and Hase,[18] in a molecular dynamics simulation at the Hartree−Fock level, observed that singlet oxygen attack on a short (5,0) semiconductor SWNT segment also forms a stable 1,4-endoperoxide; at higher energies a 1,2-dioxetane (in which O_2 adds across one C═C bond) was also found. Our 1.2 eV maximum desorption activation energy is in the range of the measured activation energies for unimolecular decomposition of (unprotonated) endoperoxides,[34] although the similarity could be coincidental. All this evidence suggests creation of an endoperoxide in our reoxygenation experiments.

Using B3LPY 6-31g* DFT methods of calibrated accuracy, we calculated 1,2-dioxetane (addition across one C═C bond) and 1,4-endoperoxide (addition across a hexagon) equilibrium structures on a short section of the (8,0) semiconductor tube with H end atom termination ($C_{64}H_{16}$). The most stable structure is the endoperoxide oriented along the SWNT axis in Figure 4b; this species is bound with respect to dissociated $^3\Sigma$ oxygen by 0.07 eV (cc-pvtz(-f)[46]). The dioxetane structure (oriented at 60° with respect to the tube axis) gives a local minimum about 0.4 eV higher. The endoperoxide transition state for concerted desorption (Figure 4a) lies 1.31 eV above the bound complex, close to the energy of O_2 in the excited $^1\Delta$ state. Both the transition state and the bound oxygen complex are in the singlet spin state. These computational results support the Mann and Hase Hartree−Fock result of endoperoxide formation by reaction with $^1\Delta$ oxygen, with an activation energy for desorption on the order of 1 eV.

What is the protonated species? The neutral endoperoxide is not stable if a proton is introduced about 1 Å from one of the O atoms. The calculation converges to two different local minimum structures, starting from different initial proton positions. The most often observed is a hydroperoxide structure shown in Figure 5a; the other is the dissociated structure consisting of an epoxide and OH in Figure 5b, which is more stable by 2.2 eV (cc-pvtz(-f) basis). However, the latter structure is expected to have a much higher activation energy for decomposition and therefore is not expected to be formed reversibly under our experimental conditions. We therefore exclude this structure as inconsistent with our experimental observations. In the neutral endoperoxide structure (Figure 4b), the Mulliken charge on the two O atoms is −0.34e, with +0.34e on the SWNT carbon atoms. In the protonated Figure 5a species, the charge on the SWNT itself is about +1.16 e, residing

(44) Bloodworth, A. J.; Eggelte, H. J. In *Singlet O_2*; Frimer, A. A., Ed.; CRC Press: Boca Raton, FL, 1985; Vol. II, Chapter 4.
(45) Sakai, K. I.; Ohshima, S.; Uchida, A.; Oonishi, I.; Fujisawa, S.; Nagashima, U. *J. Phys. Chem.* **1995**, *99*, 5909−5913.
(46) A high-level correlation-consistent polarized valence triple-ζ atom-centered basis set.

Scheme 1. Proposed Mechanism for Formation of Protonated SWNT Oxide[a]

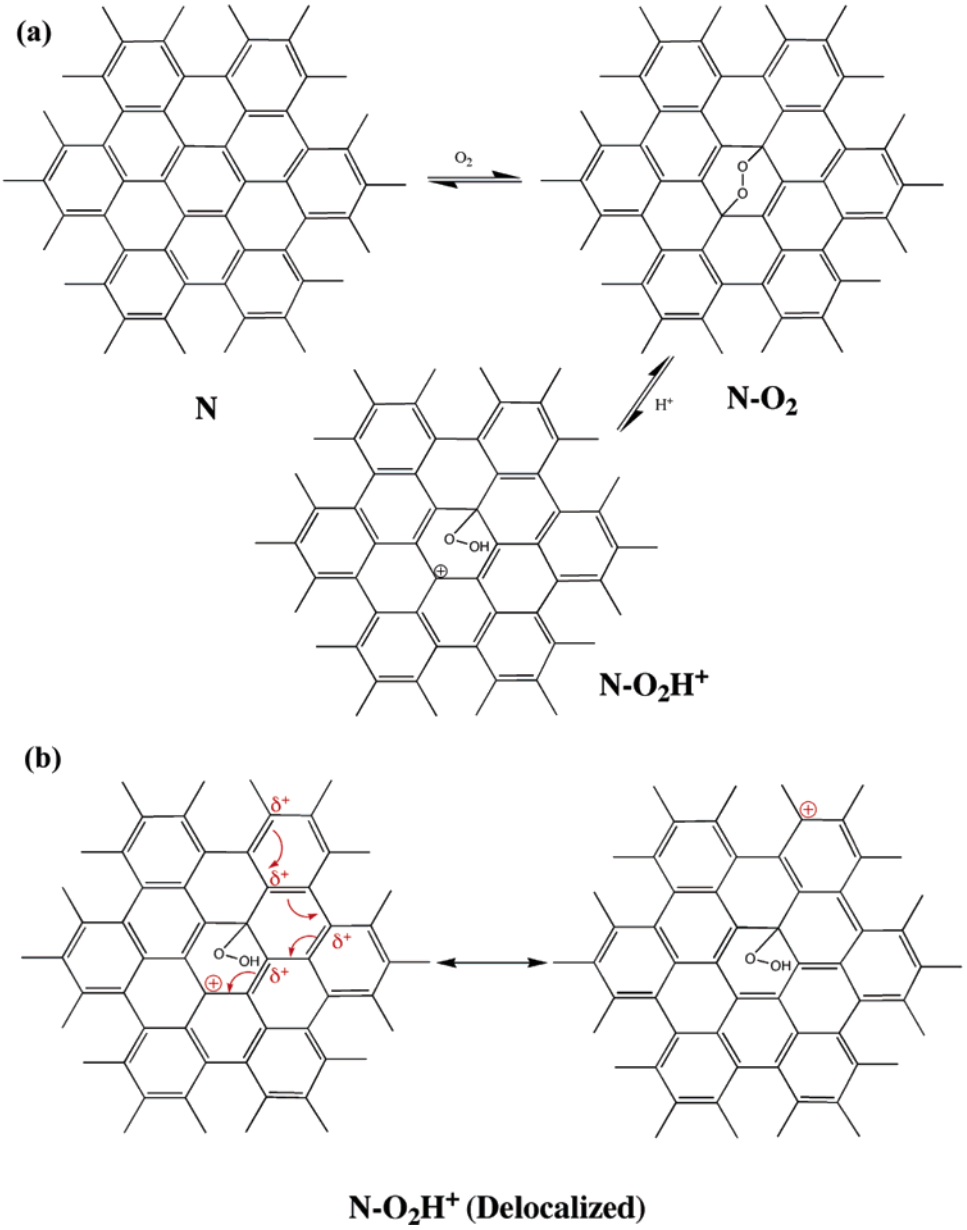

[a] (a) Formation of SWNT endoperoxide followed by protonation to form the hydroperoxide carbocation. (b) Resonance structures illustrating the carbocation stability.

principally in the tube HOMO. Note that the protonated oxide species should reside in a more water-like local environment than the neutral oxide, and this effect might alter the calculated protonated oxide structure and energetics. The SWNT length and curvature dependence of these results remains to be explored.

In Scheme 1, we propose a reaction mechanism consistent with our experimental results and calculations. The structure N represents a nanotube sidewall fragment. In the first step, one aromatic ring reacts with oxygen to produce the 1,4-endoperoxide $N\text{-}O_2$. This covalently bonded endoperoxide does not hole-dope the nanotube or affect the luminescence. Under acidic conditions, 1,4-endoperoxides of aromatic compounds are known to protonate and open the endoperoxide ring,[47] consistent with the DFT calculation results described above. Protonation of the endoperoxide forms a carbocation (structure $N\text{-}O_2H^+$), i.e., a hole in the π-system valence band. Scheme 1b illustrates that many equivalent resonance structures can be drawn for $N\text{-}O_2H^+$,[48] demonstrating the stability of the carbocation that results from delocalization. This delocalized hole is responsible for luminescence quenching by nonradiative Auger recombination. To explain the reversibility of the quenching, we postulate that the intermittent removal of protons at pH 3 causes the hydroperoxide in $N\text{-}O_2H^+$ to be transformed into a peroxide anion which snaps back to a 1,4-endoperoxide (reverse of the protonation mechanism in Scheme 1a). At 97 °C, $N\text{-}O_2$ loses molecular oxygen to regenerate $N + O_2$ (singlet or triplet), and the capacity for photoluminescence is restored. The equilibrium is shifted toward the dissociated species by removal of O_2 under

(47) Catalani, L. H.; Wilson, T. *J. Am. Chem. Soc.* **1989**, *111*, 2633−2639.

(48) Prakash, G. K. S.; Rawdah, T. N.; Olah, G. A. *Angew. Chem., Int. Ed. Engl.* **1983**, *22*, 390−401.

argon. We note that the partitioning of carbocations between internal addition of nucleophiles and protonation−deprotonation is well established.[49]

Systematic Aspects of SWNT Oxidation. The sensitivity of nanotube band-gap optical absorption and luminescence to the presence of acid and oxygen is strongly diameter-dependent. In air-saturated samples, the larger the nanotube diameter, the more sensitive its luminescence is to the presence of acid, as compared to the absorption. The difference is very large for the larger-diameter tubes in Figure 1c. We also find that the oxygen is removed most slowly from the tubes of largest diameter, and their luminescence is quenched at lower concentrations of DMN-O_2.

Both surface oxide properties and SWNT delocalization should depend on tube diameter. Calculations predict that smaller-diameter tubes form more stable dioxetane complexes with oxygen,[16,19] but the kinetics and stability of nanotube endoperoxides relative to diameter remains unknown. A hole in a nanotube, once formed, is more delocalized in the larger-diameter tubes. This is shown by the fact that the effective mass for motion along the tube axis varies inversely with the tube diameter in the simple band theory.[3] In valence bond language, the extent of resonance-based hole delocalization depends on the degeneracy of the various resonance structures. A three-fold symmetry is implicit in Scheme 1b for flat graphite; rolling the sheet into a tube lowers the symmetry and therefore partially removes the degeneracy of the different resonance forms. Tighter rolling causes larger energetic spacings between erstwhile degenerate resonance forms. Note that as the SWNT diameter increases, the band gap decreases. In bulk semiconductors, the Auger effect increases as band gap decreases.[50]

In SWNT research, tubes are typically processed and handled in air. All nanotubes can have strongly bound surface oxides resulting from sidewall damage. Are there also surface endoperoxides on tubes without damage when H^+ is not present? The equilibrium coverage of endoperoxide in air can be calculated from a Langmuir adsorption analysis, given the oxygen pressure and the binding energy. For a binding energy of 0.1 eV, we calculate that there is only one endoperoxide for every 12 μm of length at 23 °C in air. However, at 23 °C the equilibrium forms very slowly, and the equilibrium coverage may not be experimentally relevant. Surface endoperoxides form fast kinetically from $^1\Delta$ attack, if this species is available. For an average nanotube, the experimental oxide residence time at 97 °C is 18 min for a 1.2 eV activation energy; at 23 °C it would be on the order of 6 months. A long residence time at 23 °C is supported by our observation that the (luminescence quenching) surface oxide formed by $^1\Delta$ reoxidation is stable at least for several days under Ar. Thus, tubes kept at 23 °C appear to have a long memory of prior processing. Our initially prepared 400 nm long tubes apparently have hundreds of surface oxide species that can be protonated, as judged from the bleaching experiments. Moreover, all these surface oxides are experimentally in reversible equilibrium with oxygen gas at 97 °C, as judged from the luminescence recovery experiments.

(49) Richard, J. P.; Ames, T. L.; Likn, S.; O'Donoghue, A. C.; Toteva, M. M.; Tsuji, Y.; Williams, K. B. *Adv. Phys. Org. Chem.* **2000**, *35*, 67.
(50) Agrawal, G. P.; Dutta, N. K. *Long-wavelength semiconductor lasers*; Van Nostrand Reinhold Co.: New York, 1986.

Conclusion

We have quantitatively investigated optical bleaching and luminescence quenching due to hole-doping by protonated surface oxides. We propose that the surface oxide is a 1,4-endoperoxide which, upon protonation, forms a hydroperoxide carbocation that injects a hole into the π-electron valence band. We find that the SWNT band-gap luminescence is extremely sensitive to hole-doping, much more so than the band-gap optical absorption. We attribute the luminescence quenching to an Auger nonradiative recombination process.

Acknowledgment. The authors thank P. Deo and P. Somasundaran for supplying the PMAOVE and V. Perebeinos and M. Strano for informative discussions. Financial support was provided by the U.S. Department of Energy under DOE Grants No. FG02-98ER14861, FG02-90ER14162, and FG02-03ER15463, the National Science Foundation (Grant CHE-010110655, MRSEC Program Grant DMR-0213574, and Nanoscale Science and Engineering Initiative Grant No. CHE-0117752), and the New York State Office of Science, Technology, and Academic Research (NYSTAR).

Supporting Information Available: Calculation of band-gap absorption bleaching in SWNTs due to band-filling effect. This material is available free of charge via the Internet at http://pubs.acs.org.

JA046526R